LABORATORI NAZIONALI DI FRASCATI
SIS-Pubblicazioni

LNF-97/030 (P)
23 Luglio 1997

THE GRAAL HIGH RESOLUTION BGO CALORIMETER AND ITS ENERGY CALIBRATION AND MONITORING SYSTEM

F. Ghio, B. Girolami
Istituto Superiore di Sanità and INFN Sezione Sanità ,
Viale Regina Elena 299, 00161 Roma, Italy

M. Capogni, L. Casano, L. Ciciani, A. D'Angelo, R. Di Salvo,
L. Hu, D. Moricciani, L. Nicoletti, G. Nobili, C. Schaerf
INFN Sezione Roma2 and Università di Roma 'Tor Vergata',
Via della Ricerca Scientifica 1, 00133 Roma, Italy

P. Levi Sandri
INFN-Laboratori Nazionali di Frascati,
Via Enrico Fermi 40, 00044 Frascati, Italy

M. Castoldi, A. Zucchiatti
INFN Sezione di Genova and Università di Genova,
Via Dodecaneso 33, 16146 Genova, Italy

V. Bellini
INFN Laboratori Nazionali del Sud and Università di Catania,
Corso Italia 57, 95129 Catania, Italy

Abstract

We describe the electromagnetic calorimeter built for the GRAAL apparatus at the ESRF. Its monitoring system is presented in detail. Results from tests and the performance obtained during the first GRAAL experiments are given. The energy calibration accuracy and stability reached is a small fraction of the intrinsic detector resolution.

PACS:29.40.Vj

Submitted to Nuclear Instruments & Methods in Physics Research

1 Introduction

The GRAAL beam line facility [1)] currently in operation at the ESRF in Grenoble, is the first source of high intensity and completely polarized γ rays in the energy range $0.4 \div 1.5$ GeV. This project has been realized, with the prevailing support of the Istituto Nazionale di Fisica Nucleare (INFN), to study polarization observables in photoproduction reactions including strangeness.

The GRAAL apparatus (see Fig. 1), consists of a high resolution and large solid angle BGO electromagnetic calorimeter combined with multiwire proportional chambers (MWPC) that covers a solid angle range of almost 4π. Particles emitted at small angles are also detected by a scintillator wall, that is installed three meters from the target and permits particle identification by means of their time of flight and their energy loss in the scintillators. The particle identification in the central region is accomplished with a plastic scintillator barrel through the measurement of dE/dx.

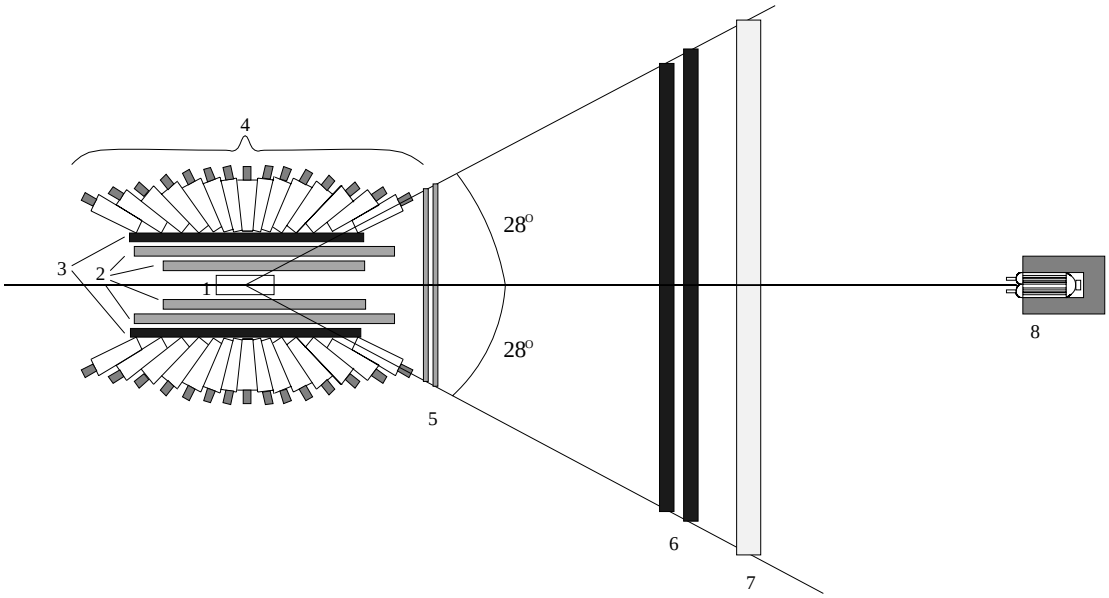

1) Liquid hydrogen target
2) Cilindrical wire chambers
3) Plastic scintillators barrel
4) BGO crystals
5) Plane wire chambers
6) Double scintillators wall
7) Sandwich calorimeter
8) Beam monitor

Figure 1: Layout of the GRAAL apparatus.

In this paper we describe the photon-detection system, which has been designed to measure the energy of γ and neutral mesons decaying in two or more photons (π^0, η, η', K^0, ϕ), with a good angular resolution. The calorimeter covers 90% of the entire solid angle, detecting particles emitted at angles from 25° to 155°.

The accuracy and reliability of the energy calibration is a basic requirement for this

detector in which a large number of BGO sectors, comprising about 500 PMs, are involved and high resolution is expected. The problem is to keep under control the variations in the gain and temperature of the different sectors as a function of time, thus ensuring uniformity of response during data taking and keeping to a minimum the time spent calibrating the calorimeter. We shall, therefore, give particular emphasis to the description of our LED-based monitoring system, which plays a key-role in this respect.

In sect. 2 we describe briefly the characteristics of the apparatus. In sect. 3 the principles of the electronics and data acquisition. Sect. 4 is devoted to the calibration procedure. The gain monitoring system is described in sect. 5. In sect. 6 we report on the linearity of the calorimeter energy response. In sect. 7 we report on the performances of the BGO calorimeter and the monitoring system, with special emphasis on the energy resolution and time stability.

2 Description of the detector

The BGO detector is shown in detail in fig. 2. The mechanical support structure consists

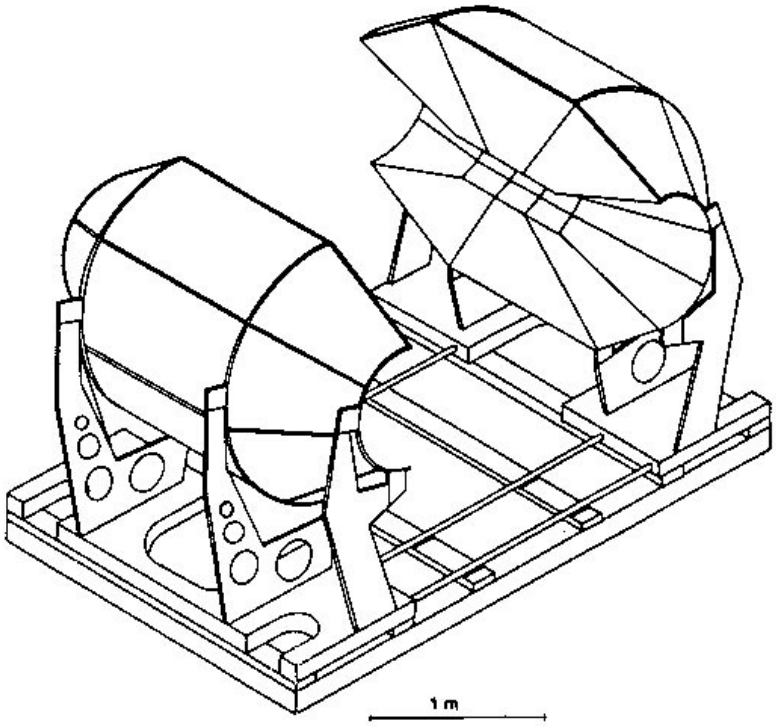

Figure 2: A sketch of the BGO calorimeter showing the carbon fiber baskets mounted on the external support frame separable into two halves.

of 24 baskets of Carbon fiber composite material supported by an external steel frame. Each basket is divided into 20 cells with very thin walls, 0.38 mm for the inner and 0.54 mm for the outer walls, to keep the crystals optically and mechanically separated. The Carbon fiber has been preferred to other materials like Aluminum for its higher rigidity and lower gamma ray attenuation due to its low Z number. The support frame is divided into two halves which can be taken apart by 1.5 meters to allow access to the target and central detector region. When closed the structure leaves a 20 cm diameter hole along the beam-line for the insertion of the target, the cylindrical wire chambers and the plastic scintillator barrel.

The crystals are of 8 different dimensions and are shaped like pyramidal sectors with trapezoidal basis [2] (see fig.3). They define 15 angular regions (ϑ) in the plane

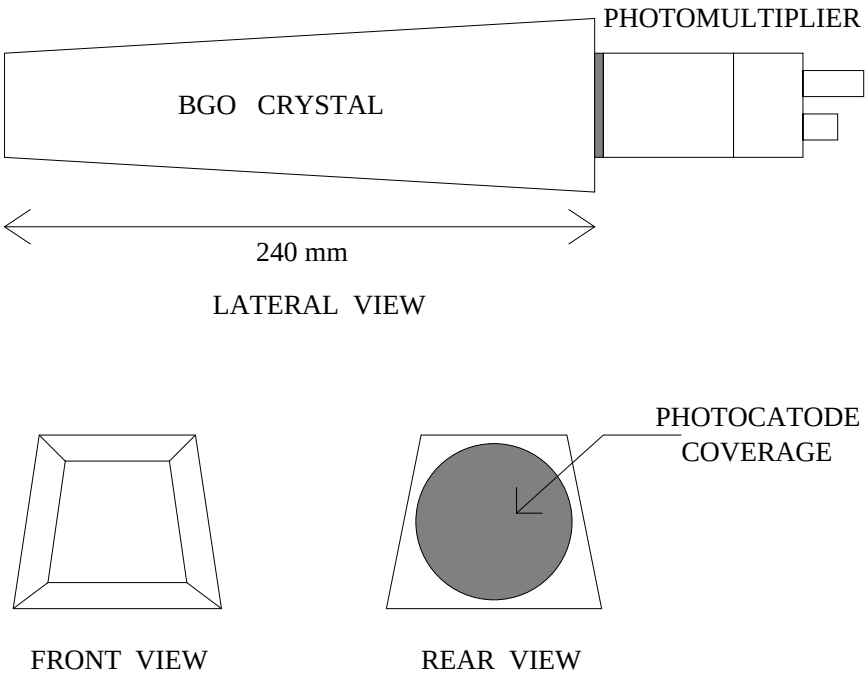

Figure 3: Schematic views of a BGO crystal.

containing the symmetry axis of the calorimeter, coincident with the beam axis, and 32 (φ) in the plane orthogonal to the beam axis (see Tab.1 of [3] and [4] for details). The 480 crystals have all the same length of 24 cm ($>$21 radiation lengths), for a good confinement of photon showers in the GeV region, and are arranged in such a way that the reaction products emitted in all directions from the target center encounter a constant thickness of BGO. Each crystal is wrapped up in a thin (30μm) aluminized mylar reflector, and its back side is optically coupled to a photomultiplier (PM) [5]. Two holes in the back side of the crystal support are used for monitoring the temperature and for the input, through

optical fiber, of light pulses which are used for the measurements of the linearity and gain stability of the photomultipliers.
During the production phase each one of the crystals has been accurately tested to check the accomplishment of the requirements imposed for acceptance: longitudinal uniformity $\geq$ 95% and resolution at the 0.661 MeV Cesium γ-peak $\leq$ 20% FWHM. The quality tests gave results better than the design specifications. Two thirds of the crystals have an average resolution at Cesium better than 18% FWHM and two thirds have a longitudinal uniformity greater than 97%.

3 Electronics and data acquisition

3.1 The linear chain

Since the BGO calorimeter is operating in a region without magnetic field and we need to measure with a good resolution electromagnetic showers with energy less than few hundreds MeV, we choose for the readout of the signal standard photomultipliers due to their noise much smaller than that of other devices such as photodiodes.

The anode signals from the PMs enter in 15 adders (MIXER), each having 32 input channels with programmable attenuators [6]. The outputs from each module consist of : a linearly summed prompt output, with a fan-out of 6, used for trigger purposes and to build up the calorimeter total energy hardware sum. A 300 ns delayed and, if necessary, attenuated output that is sent for digitization to two FERA modules (Fast Encoding and Readout Adc, charge-sensitive, 11-bit, 16 channels per unit) [7]. The linearly summed output of each MIXER (Σ_ϑ) corresponds to the sum of the signals coming from the 32 BGO crystals having the same ϑ angle. The 15 Σ_ϑ outputs are sent to another MIXER

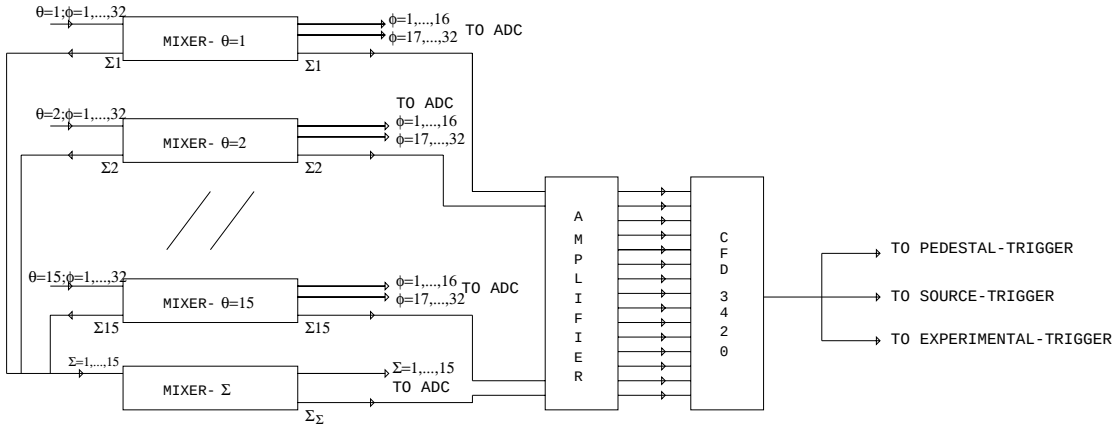

Figure 4: Scheme of the linear chain of the electronics.

(MIXER-Σ). The individual linear output signals from the MIXER-Σ are sent to another FERA ADC for the acquisition of the partial sums. The summed output signal from the MIXER-Σ, that corresponds to the total energy of the BGO calorimeter, is sent to the different trigger circuits and to another FERA channel (see fig. 4). The linear part of the acquisition electronics is thus formed by 16 MIXER and 31 FERA ADC modules.

3.2 The readout system

For the ADC read-out of the BGO calorimeter and other detectors of the GRAAL apparatus we have found an original solution that allow a fast and sequential acquisition of all the CAMAC Crates using the FERA-BUS. In fig. 5 is shown the scheme of the handshake logic for the read-out of the ADC. The FERA ADC of each crate are connected

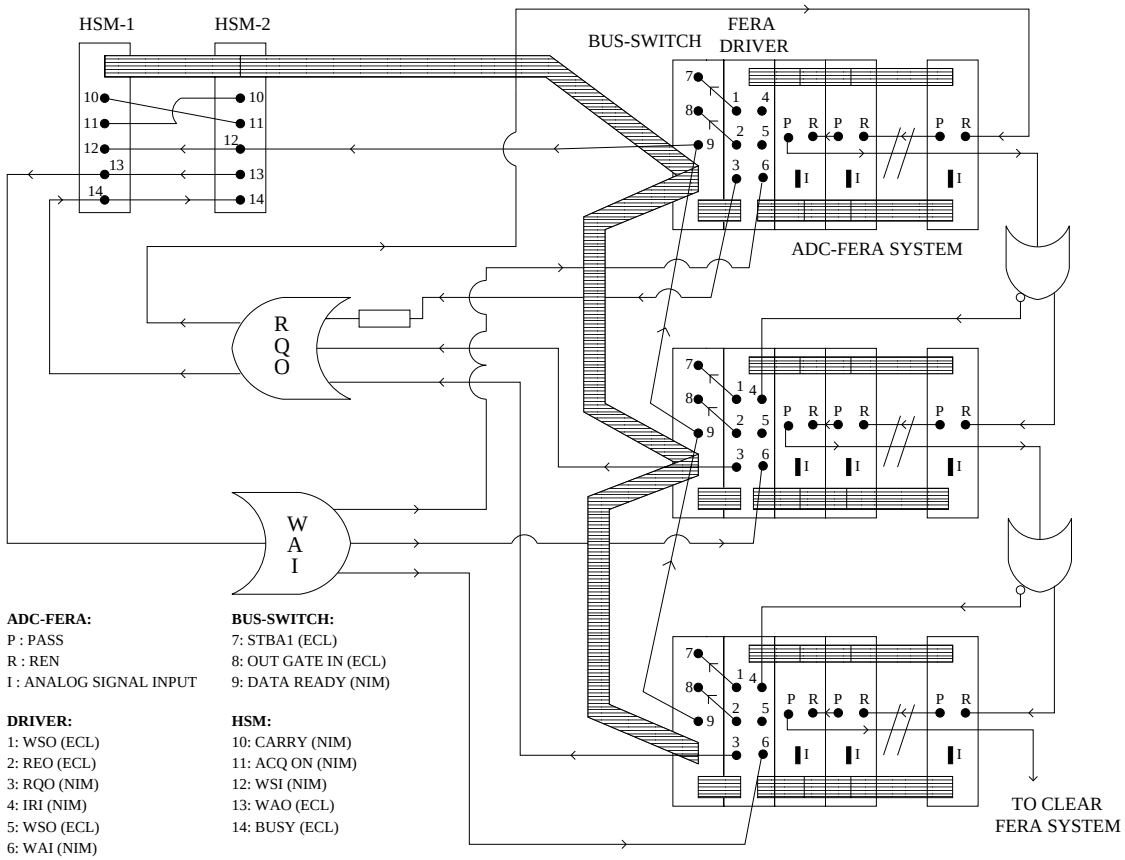

Figure 5: Scheme of the read-out system and handshake logic.

in parallel to the FERA-DRIVER [8)] through the COMMAND-BUS and the DATA-BUS. We have specifically designed a system that needs only one BUS for the data coming

from the DRIVERS of each Crate. For this purpose we have used three BUS-SWITCH modules [9] as interfaces between the FERA-DRIVERS and the single DATA-BUS. The BUS-SWITCH module was originally designed to accept as input the signals from two different DATA-BUS giving at the output one of the two depending on the status of the strobe signals of the two DATA-BUS. In our scheme we exploit the three state port characteristic of the BUS-SWITCH output. The open circuit state of the output allows to disconnect the module from the BUS, in such a way that the transmission on the same BUS of signals from other modules is not disturbed. Using one BUS-SWITCH module for each crate and connecting the DRIVER data output with one of the two BUS-SWITCH data inputs, with a suitable signal timing logic, we achieve the "mixing" of the data on a single BUS. The FERA-ADC are sequentially read starting from the third Crate and continuing with the ADC of the second and first Crate pertaining to the BGO calorimeter. During the calibration phase the data are temporarily stored in an auxiliary memory area formed by two High Speed Memory modules [10] HSM-1 and HSM-2, as shown in fig.5. These memories are configured to work in a flip-flop to combine acquisition and data readout without loss of speed. When HSM-2 is filling, HSM-1 transfers the recorded data to the memory of the calibration processor [11], according to an Interrupt scheme, and will be ready to accept new data when HSM-2 is full.

During the experimental data acquisition the gate signal for the FERA-ADC is given by the experimental trigger and the FERA-BUS is automatically connected to the general data-bus for the global acquisition of all the detectors of the GRAAL apparatus.

4 The calibration and equalization method

The absolute calibration of the crystals is obtained using the 1.27 MeV photons (E_{source}) from a ^{22}Na source. The response of the 480 BGO sectors is equalized using an automatic procedure, that sets all the PM's gains, varying their high voltage. If we call c_{eq} the calibration channel we would like to obtain, we can say that the equalization is achieved when all the ADC channels c_i ($i = 1, \ldots, 480$) are within the following range:

$$\frac{|c_i - c_{eq}|}{c_{eq}} \leq B(\%)$$

$B(\%)$ indicates the precision of the procedure. To maintain the time spent for the equalization at the reasonable value of about one hour, we fix $B = 1.5\%$. This value affects only the precision on the hardware energy sum used for the experimental trigger, but does not affect the absolute calibration resolution because in the data analysis the exact value of the calibration constant for each crystal is used.

The choice of the equalization channel is determined by the maximum energy value that has to be measured and by the range of the detector linearity response. The maximum γ energy of the GRAAL beam is 1.5 GeV, but the Monte Carlo simulations and the experimental data [12] indicate that no more than 80% of the incident γ energy can be contained in a single crystal ($E_{max} = 1.2$ GeV), due to the transverse spread of the electromagnetic shower. The saturation effects of the crystals PMs become evident for peak pulse amplitudes of the order of 5 V, so that the signals corresponding to the maximum energy released should not exceed this value. For the signals coming from BGO scintillation events, we have measured the following relation between the peak amplitude of the signal V_{peak}(mV) and the ADC channels:

$$V_{peak} = 10 \text{ mV} \;\Rightarrow\; 100 \text{ channels}$$

The end-scale value of our FERA-ADC is 1920 channels, corresponding to a signal equivalent charge of 480 pC. To this value we must subtract the channels corresponding to the pedestal signal, that have been adjusted in the range 100-120; for this reason we can assume that the maximum number of ADC channels available is: $c_{e-s} = 1800$. In the hypothesis of a linear response, the following relation holds:

$$E_{max} = \frac{c_{e-s} \cdot E_{source}}{c_{eq}} \cdot \frac{1}{f} \tag{1}$$

where f is the attenuation factor on the analog signal introduced by the MIXER. According to (1), we obtain in our case:

$$c_{eq} \cdot f = 1.91 \tag{2}$$

The best value for f is determined knowing that the V_{peak} values of the signal corresponding to c_{e-s} depend on the attenuation factor, according to the following relation:

$$V_{peak}(\text{mV}) = \frac{c_{e-s}}{f} \cdot 0.1 \text{ mV/channel} = \frac{180 \text{ mV}}{f}$$

from which we decided to use $f = 1/32$, that represents the best approximation between the available attenuation factors. From eq.(2) it follows that c_{eq}=64 is a reasonable compromise between calibration precision and saturation effects. This way, without attenuation, we obtain a calibration constant m_{eq} $\simeq$0.02 MeV/channel. The maximum energy that can be measured with attenuation is thus equal to $\simeq$1.15 GeV compatible with the expected E_{max} value.

5 The calibration monitoring system

5.1 Introduction

The calibration constant of each crystal measured at the equalization time t_0 may change as a function of time, due to two principal reasons: variation in the crystal light output due to temperature effects and variation in the PM gain.

To control the temperature effects we have set up a monitoring system, that is discussed in details in [13] and will not be described further here.

Gain variations of the photomultipliers may occur as a consequence of the following effects:

- photocathode temperature variation: at the BGO peak emission wavelength (480 nm) the efficiency variation of a bialkali photocathode is of the order of -0.4%/°C;
- instability in the high voltage power supply [14]: these are of the order of ± 1 V and assuming a HV typical value V=1500 V, the induced gain variations are 0.6% for the R580 PM model and 0.8% for the R329-02 model; during the acquisition of the calibration peaks, this effect is however strongly reduced as it is averaged over a long time interval;
- PM drifts and shifts; for both source and experimental events, we have an anodic mean current of the order of 10^{-2} μA, much lower than the maximum value of 1 μA recommended in order to avoid drift effects; also shift effects can be neglected as previous tests made on a basket of 20 BGO crystals [12] have shown that for rates lower than 1 KHz, as in our case, we have a gain variation due to shift effects of the order of 0.01%;
- aging of cathode and dynodes materials: a typical time scale for these effects is of the order of few years and can be kept under control with a regular monitoring of the PMs gains;
- voltage dividers instability: this effect does not cause a time variation of the PM gain but a loss of linearity in the PM response; the linearity curves have been measured as reported in section 6.

In order to keep under control all time variations of the calibration constants previously discussed we have realized a photomultiplier gain monitoring system as described below.

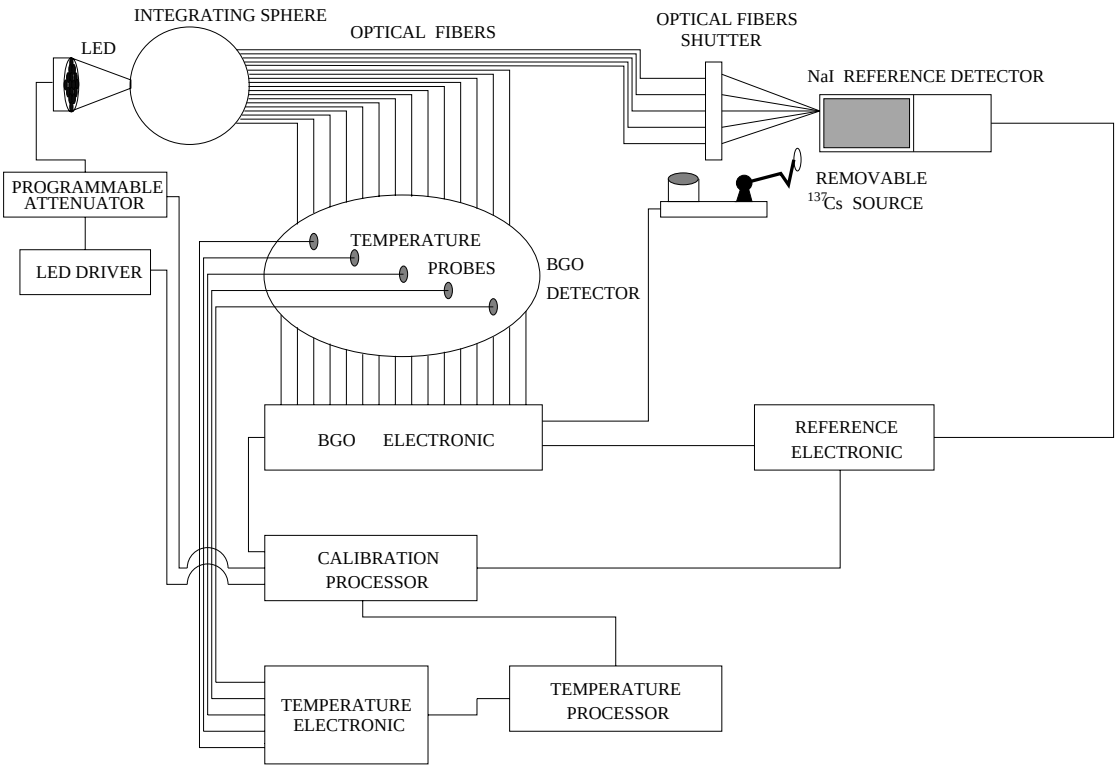

Figure 6: Schematic view of the calorimeter gain and temperature monitoring system.

5.2 The photomultiplier gain monitoring system

The monitoring system, as shown in fig. 6, is made of:

- high luminosity, blue emitting, pulsed LEDs as light source;
- a light distribution system consisting of an integrating sphere and optical fibers;
- a reference NaI scintillation detector.

A matrix of 7 LEDs [15], is directly coupled to the input port of the integrating sphere. The following aspects were taken into account with particular care in the final choice of the light source:

- emission spectrum;
- time stability;
- time shape of the light pulse;
- intensity.

The emission spectrum of the chosen LEDs has a maximum at 450 nm with a FWHM of 140 nm, that is quite similar to the BGO one.

The LED pulse-to-pulse stability is of the order of 1%, depending on the light intensity. In fig. 7 is shown the LED pulse distribution corresponding to the maximum light intensity, in a generic BGO crystal. Measurements done in a time interval of several days have shown that the LED time stability is of the order of a few percent.

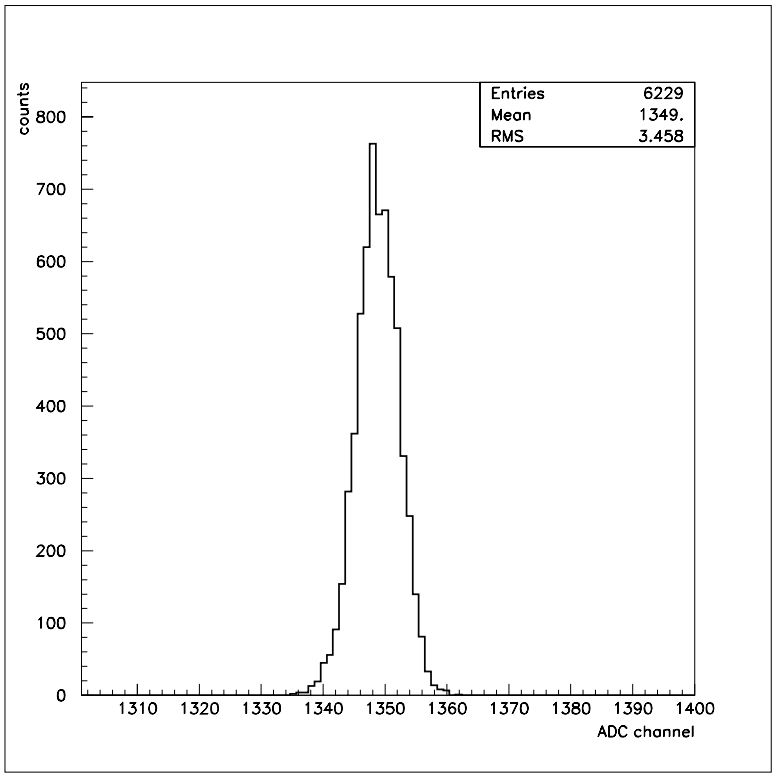

Figure 7: LEDs pulse to pulse stability distribution.

We decided not to use the pulsed laser source [16], in spite of its high intensity, because it had a pulse to pulse instability greater than 20% (FWHM) and showed a time drift in the emission intensity as high as 50%.

The time shape of the light pulse is important for two fundamental reasons. The first is that the PM anode pulse from the light source should reach a charge equivalent to $\sim$1 GeV energy without having a current peak that gives rise to saturation in the PM. The second reason is that the PM response may depend on the time shape of the input pulse also without saturation effects. Especially for these reasons we realized a driver circuit for the LEDs that produces an anode pulse, see fig. 8, very similar to that produced by scintillation in BGO.

The intensity of the light source should be high enough to simulate the maximum energy deposited in each detector. The actual configuration of the LEDs produce an equivalent energy of almost 1 GeV for each of the 480 BGO crystals.

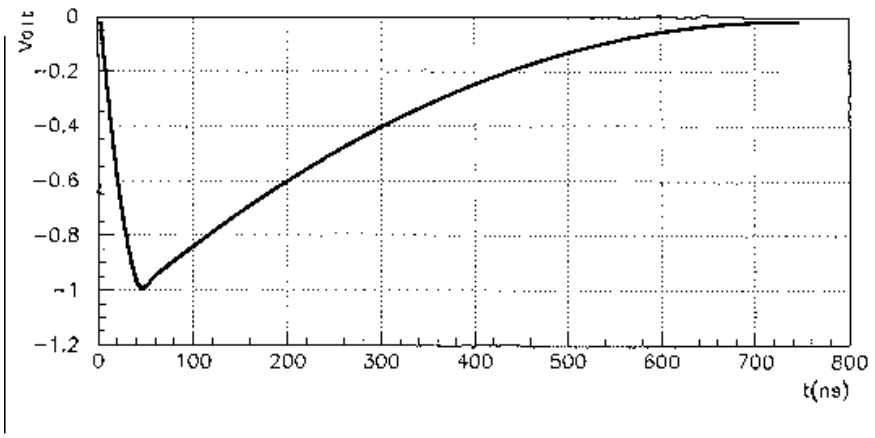

Figure 8: Anodic pulse shape generated by the LEDs driver circuit.

We have chosen an integrating sphere of 6" internal diameter [17] to match the LEDs light to the 600 optical fibers, 6 meters long, carrying the light to each detector. This solves in a simple way the challenging problem of having a uniform light distribution over the fibers that are connected to the exit port of the sphere. Thus the ratios of the incident light intensities over any couple of fibers are constants independently of the variations of the light source. The inner surface of the sphere consists of Spectralon reflectance material that gives the highest diffuse reflectance of any known material over the UV-VIS-NIR region of the spectrum. The reflectance is generally $>$99% over the range 400-1500 nm. Radiation introduced into the sphere undergoes multiple scattering, which results in a uniform, spatially integrated radiation distribution within the sphere. The exit port serves as a source of radiation characterized by a radiance which is constant over the plane of the exit port and independent of viewing angle. The light carried by each fiber is then optically coupled to each crystal.

The reference detector is a crucial part of the linearity and gain monitoring system because it measures the intensity of the light pulses from the LEDs and the outputs of all the other detectors are compared to this value. Thus its linearity and gain variation should always be under control. This detector is a 2"x2" NAI(Tl) scintillator [18] coupled to the same type of PM used for the bigger BGO crystals. Five optical fibers carrying the LEDs light are coupled to the detector through a quartz window. A ^{137}Cs radioactive source was used to monitor the gain drift of its response. We have realized a system to remotely

remove the source when the LEDs light is flashing to avoid that random coincidences between the LEDs and the source signal alter the measure of the LEDs intensity.

The electronic chain and trigger circuit for the acquisition of the reference detector are different from those of the calorimeter. The anode signal is formed by a preamplifier and a spectroscopy amplifier and is then digitized by a High Performance Buffered Spectroscopy ADC [19] with 8000 channels. The data from the ADC are sent via an external bus to an Histogramming Memory [19] and at the end of the acquisition are transfered to the calibration processor memory for analysis.

6 Correction of non-linearities

Our method of calibration of the BGO calorimeter, as described in section 4, is simple, fast and very effective, allowing to determine the absolute calibration constants of all the cristals in less than ten minutes during a pause of the experimental data taking, tipically a new injection of the electron beam in the ESRF. Nevertheless the extrapolation of the calibration constant from the 1 MeV region of the gamma source to the 1 GeV region of the maximum energy deposited in a single cristal requires careful account of the possible non-linear behaviour of the electronics chain (PMs, MIXER and FERA ADC) in this large energy range. We have thus measured the linearity curve of each crystal of the calorimeter and applied these correction factors to the measured energy.

The variations of the light intensity of the LEDs over almost 3 orders of magnitude was obtained attenuating the driving LEDs input pulse using a CAMAC programmable attenuator [20] with steps of 0.25 dB. The relative intensities of the light pulses for each crystal were normalized to the response of the reference detector, the excellent linearity of which has been repeatedly verified.

6.1 The measurement of the reference detector linearity

The measure of the NaI reference detector linearity is crucial and preliminary to that of the BGO detectors. We set up a system that allows to send to the reference the light of any combination of five fibers. The five fibers coming from the integrating sphere are in fact coupled to other five fibers carrying the light to the reference in such a way that it is possible to adjust the distance between each pair of coupled fibers and thus adjust, for each fiber, the light reaching the detector. Moreover a remotely controlled shutter placed between each couple of fibers enables or disables the optical contact.

Two out of five couples of fibers are adjusted in such a way that they send the same amount of light to the reference. The output of the reference detector is measured three times : when one shutter is open, when the other one is open and when both of them are

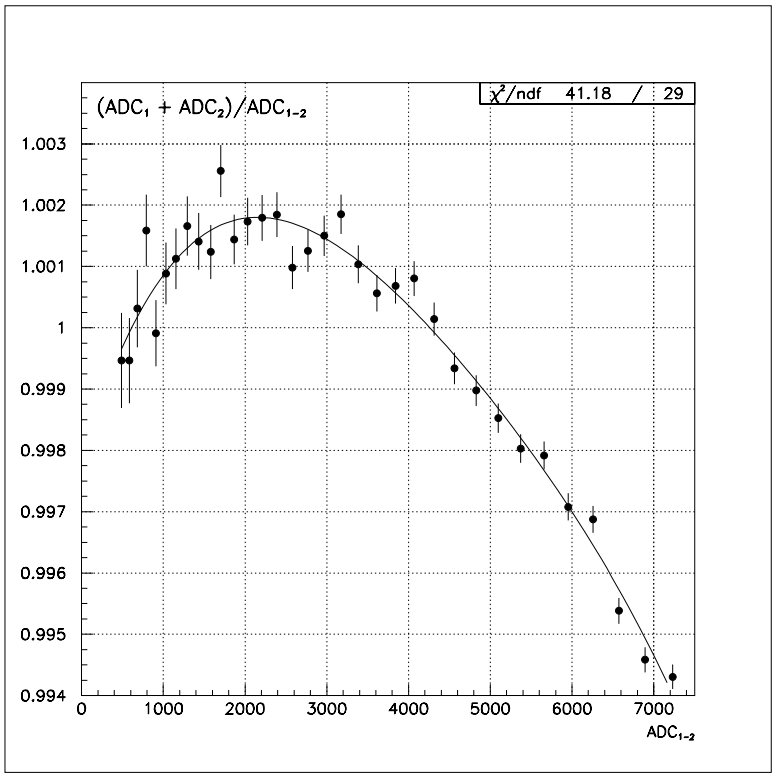

Figure 9: Ratio between the sum of the ADC channels corresponding to the two single fibers (ADC_1+ADC_2) and the channel obtained when the shutters of the two fibers were both opened (ADC_{1-2}).

open. If the system is linear the sum of the individual measurements should equal, for any light intensity, the response when both shutters are open. The variations of the LED light intensity during the three measurements, of the order of few tenths of percent, are monitored and corrected using the light measured by one BGO detector. In fig. 9 it is shown the ratio between the sum of the ADC channels corresponding to the two single fibers and the channel obtained when the shutters of the two fibers were both opened. Each point represents the linearity of that ADC channel respect to its half. These points are then fitted with a polynomial as shown in the same figure. From this curve, moving in steps of a factor of two, we can deduce the integral non linearity points of fig. 10. This figure indicates that the non linearity does not exceed $\pm 0.3\%$ in a range larger than a factor of 30. These data are fitted again with a polynomial function to obtain the curve shown in fig. 10. Applying this correction to the original points of fig. 9 we obtain the distribution of fig. 11 which indicates that, after correction, the distribution of the individual measurements is better than $\pm 0.1\%$.

With this procedure we can measure the linearity of the BGO over a factor of 30

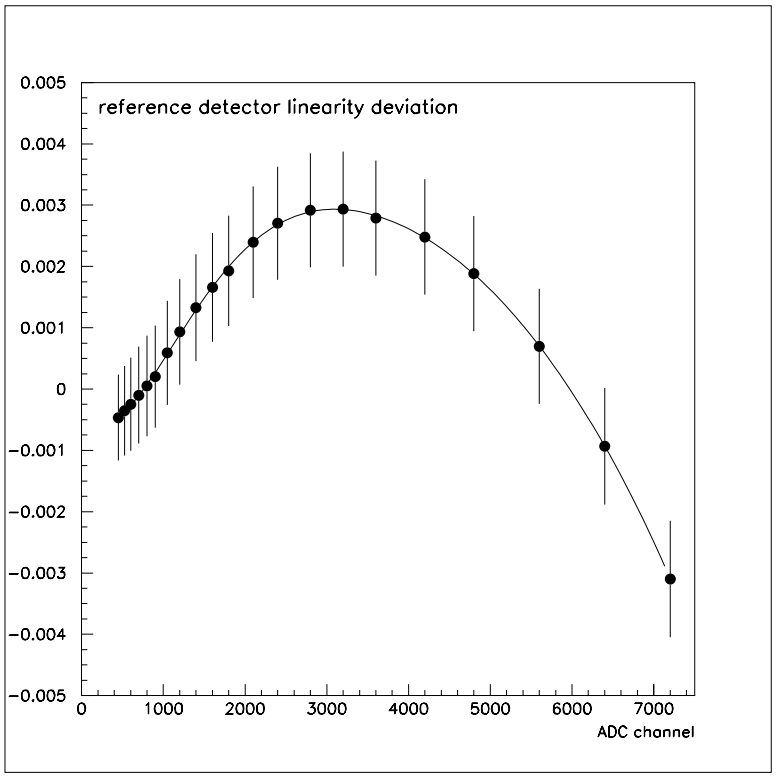

Figure 10: The integral non-linearity distribution of the reference detector respect to the channel 200.

extending approximately from 1 to 30 MeV. To extend our measurements of a further factor of 30 to arrive, in the BGO, at a light pulse equivalent to around 1 GeV, we shut off four of the five optical fibers delivering the light pulse to the reference detector. The only fiber left open had been previously adjusted to carry about 1/30 of the total light. This way the pulse in the reference detector returns to around channel 200. Increasing further the light of another factor of 30, up to its maximum value, we can extend our measurements over three orders of magnitude. This way the absolute calibration done with the ^{22}Na source at 1.27 MeV is extended up to 1 GeV. The result is a calibrated light source which covers a range of 1000:1.

6.2 The measurement of the BGO detectors linearity

In order to correct the non linear response of the BGO detectors, we developed an automatic procedure to build the linearity curves for each crystal. The LEDs light intensity has been initially adjusted in such a way to correspond to an energy of $\sim$1.27 MeV around the ADC calibration channel 64, with no attenuation. Successively a 30 dB attenuation on the analog signal is inserted and the LEDs light is progressively increased until the

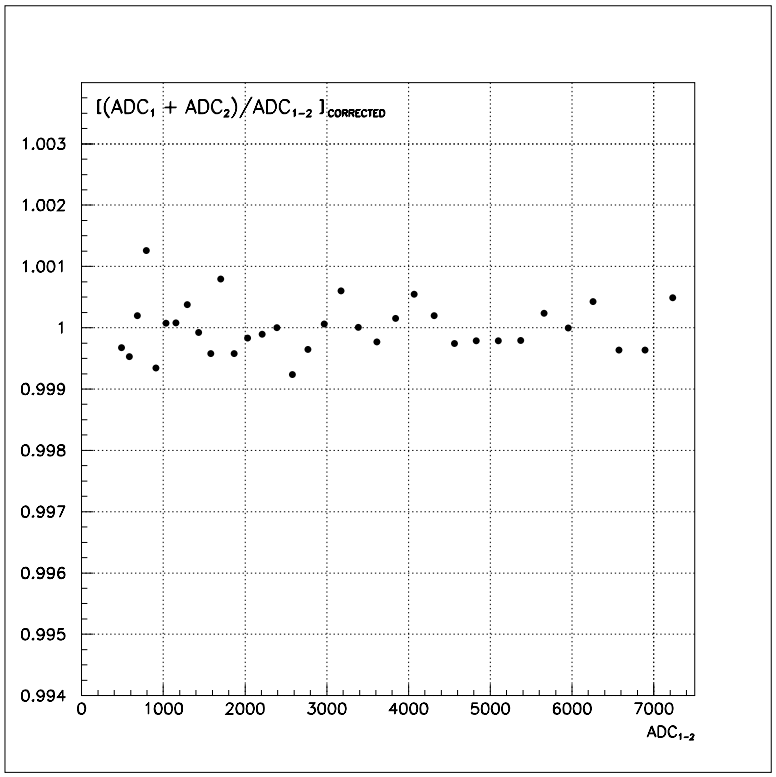

Figure 11: Same distribution of fig. 9 after the correction of the points with the non-linearity curve of fig. 10.

maximum intensity corresponds to an equivalent energy of almost 1 GeV.

This way we obtain the response of each BGO detector to light pulses of known amplitude corresponding to energies up to 1 GeV. Two typical response curves from two photomultipliers of different type are indicated in fig. 12. They have been taken with an attenuation of 30 dB. Each distribution was separated in three regions and each region fitted with a polynomial function up to the eighth degree. The energy correction factor for each ADC channel of each crystal has been extracted from these functions.

The absolute energy calibration of the ADC scale for each BGO detector with the 30 dB attenuation is obtained calculating the energy corresponding to the first point of the linearity distribution at 30 dB. This is done, for each BGO crystal, multiplying the energy calibration by the ratio between the light measured in the reference, in correspondence to this point at 30 dB, and that corresponding to the calibration channel at 0 dB.

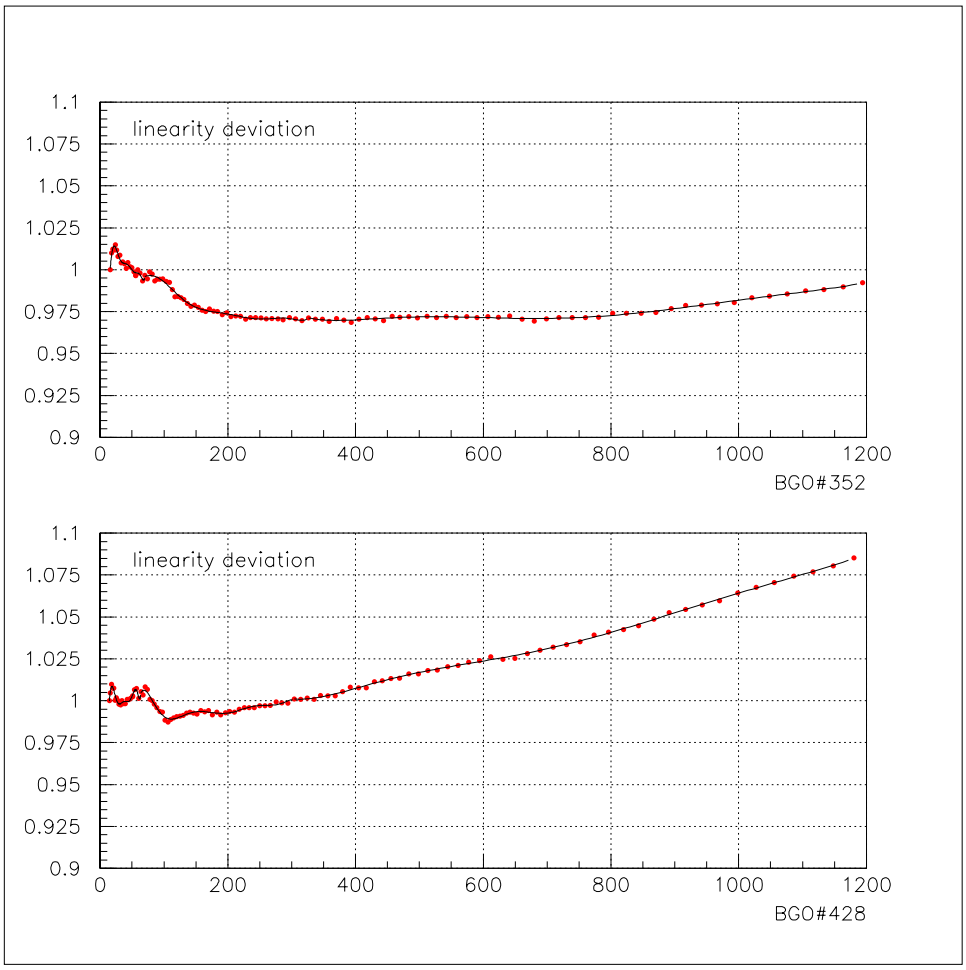

Figure 12: Two typical linearity deviation distribution corresponding to the two types of photomultipliers used for the BGO calorimeter.

7 The BGO calorimeter performances: energy resolution and time stability

The validity of the calibration method and the linearity correction procedure for the BGO calorimeter have been recently tested using the first experimental data obtained with the polarized and tagged GRAAL γ ray beam incident on a liquid hydrogen target placed at the center of the calorimeter.

In particular we looked at the reaction $\gamma + p \rightarrow \eta + p$. In order to identify the η mesons we selected the events with two neutral clusters in the calorimeter, corresponding to the decay $\eta \rightarrow 2\gamma$. We required also no charged cluster in the calorimeter and one charged particle in the forward scintillator wall, corresponding to the recoil proton. In fig. 13a and 13b are shown the reconstructed η mass distribution with and without the BGO linearity corrections. The value of the η mass has been deduced using the energy of the

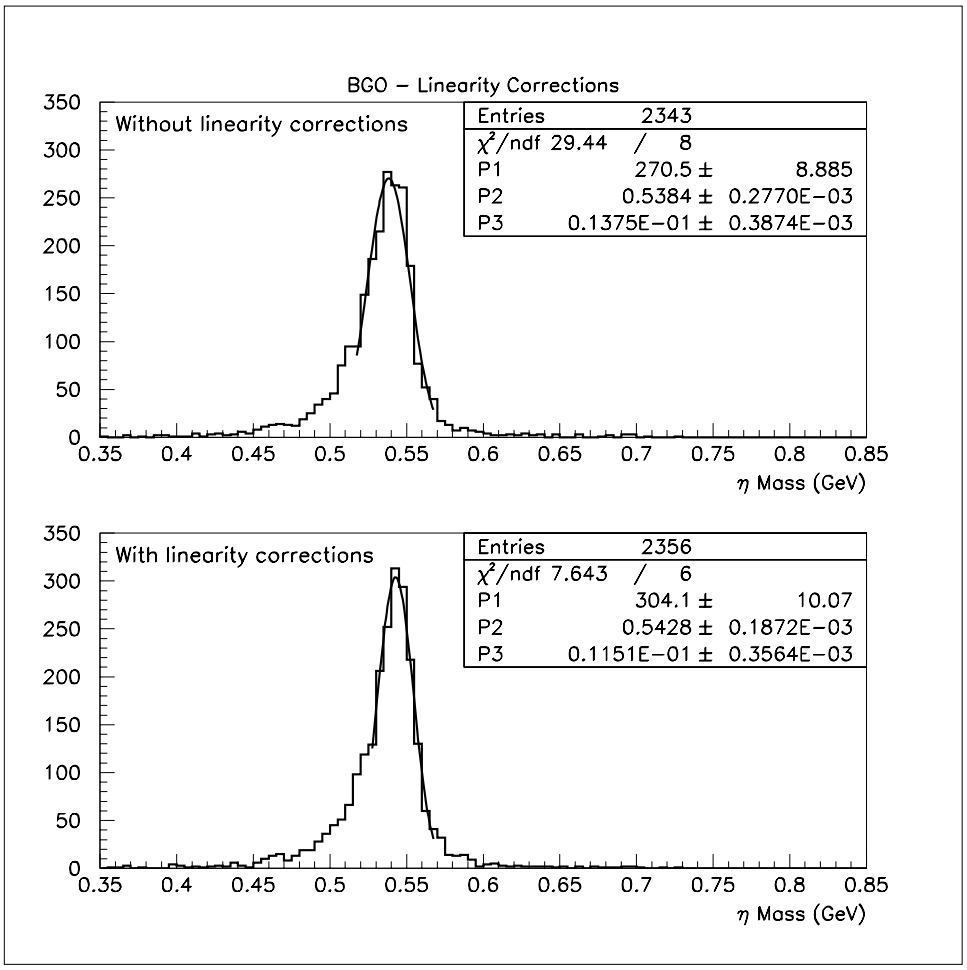

Figure 13: Reconstructed η mass distribution with and without the BGO linearity corrections. P1, P2, P3 are the parameters of the gaussian fit.

two neutral clusters, the incident γ energy from the tagging system and the angle of the proton in the forward scintillator wall.

The two distributions in fig. 13 have been fitted with two gaussian functions and their parameters are reported in the figures, where P2 corresponds to the mean value and P3 to the σ of each gaussian.

From these figures we can see that the linearity corrections increase the η mass by $\sim$ 1% and improve the resolution of the mass distribution by almost 20%.

This way the η mass distribution has a mean value of 542.8 MeV that differs by less than 1% from the true value (547.45 MeV), due to uncertainties on the incident γ ray energy and on the corrections introduced by the Monte Carlo simulation. The value of the η mass and its resolution, comparable to that measured for the BGO at these energies [12], proves the validity of this method of calibration.

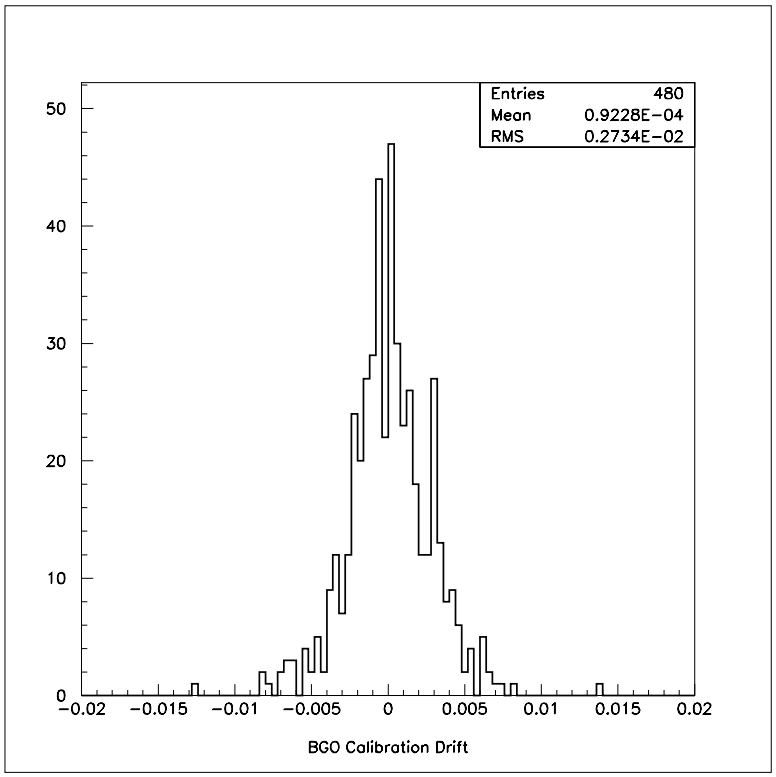

Figure 14: Drift distribution of the calibration peaks for all the BGO detectors in a time interval of 12 hours.

A typical drift distribution of the calibration peaks for all the BGO detectors, corresponding to two consecutive calibration runs, is showed in fig.14, where we can see that in the time interval of 12 hours the peak positions are stable at a few tenths of a percent level.

8 Conclusions

We have designed and installed a calibration and monitoring system for the BGO electromagnetic calorimeter in operation at the GRAAL beam of the ESRF facility.

The calibration of the entire calorimeter is done in less than ten minutes during a pause of the experimental data taking, tipically twice a day during machine injection.

We have developed a method for the correction of the non-linearity that allows the measure of the energy in a range of three orders of magnitude with an accuracy that is a small fraction of the intrinsic detector resolution.

The calibration monitoring and the linearity corrections allow to control the energy response of the calorimeter for all the data taking period at better than one percent.

9 Acknowledgements

We wish to thank the following technical staff: F. Basti, A. Orlandi, W. Pesci, G. Serafini and A. Viticchié of INFN Frascati National Laboratory; E. Tusi, L. Distante, E. Reali and M. Travaglini of University of Roma 'Tor Vergata' for their contribution to the realization of the BGO calorimeter, and the Graal collaboration for providing the data on the η photoproduction.

We are also indebted with M. Albicocco and R. Cardarelli for their precious help in designing and constructing prototypes of electronic modules.

References

1. The GRAAL Collaboration, Report ISN 9331 (Grenoble).
2. The crystals were manufactured by Quartz & Silice (De Meern, Holland) and Crismatec (Gières, France)
3. The BGO Collaboration Progress Report 1990, LNF-90/084(R)
4. A. Zucchiatti et al., *Nucl. Instr. and Meth.* **A317** (1992)492
5. Photomultiplier tubes R580 (38 mm diameter) for the 192 smaller crystals and R329-02 (52 mm diameter) for the 288 bigger ones, both manufactured by Hamamatsu Photonics. These type of PMs have been chosen after a detailed comparative test with other models; see [3)] for details.
6. CAEN Mod. SY493 based on our prototype.
7. LeCroy Camac Model 4300B
8. LeCroy Camac Model 4301
9. CAEN Mod. C 217
10. CES Mod. HSM 8170 High Speed ECL FERA bus triple port memory
11. CES Mod. FIC 8232 Fast Intelligent Controller
12. P. Levi Sandri, et al., *Nucl. Instr. and Meth.* A370 (1996) 396-402
13. M. Castoldi, et al. *The temperature monitoring system of a BGO calorimeter* submitted to *Nucl. Instr. and Meth.* Register number: CERN-97-099

14. CAEN Mod. SY403, 64 Channel H.V. System
15. MARL-OPTOSOURCE Mod. 100015, 3 mm high intensity blue LEDs
16. ADLAS (Advanced Design Laser), Germany, Diode pumped solid state laser, Q-switched, Mod. 301QD
17. produced by Labsphere, North Sutton, NH 03260, U.S.A.
18. produced by Scionix Holland
19. LeCroy Camac Model 3512 and LeCroy Camac Model 3588
20. CAEN Mod. N147, especially modified for our purposes